



Supplementary Information for

A Sos Proteomimetic as a Pan-Ras Inhibitor

Seong Ho Hong,^{a†} Daniel Y. Yoo,^{a†} Louis Conway,^b Khyle C. Richards-Corke,^a Christopher G. Parker,^b and Paramjit S. Arora^a

^aDepartment of Chemistry, New York University, New York, NY 10003. ^bDepartment of Chemistry, The Scripps Research Institute, Jupiter, FL 33458

This PDF file includes:

Figures S1 to S12
Scheme S1
Tables S1 to S6

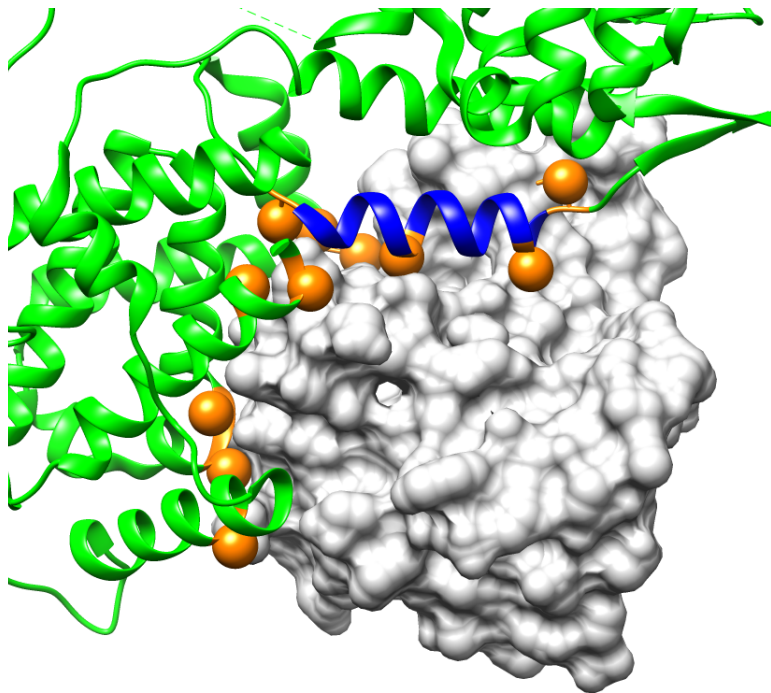


Figure S1. Alanine scanning mutagenesis of the Ras (light gray)-Sos (green) complex reveals critical Ras binding residues (orange spheres). Although, the energetically important binding residues are dispersed over the large Sos surface, the α H helix (blue) contains a cluster of these residues thereby providing a lead helical domain for rational design of Ras ligands. (PDB: 1NVW).

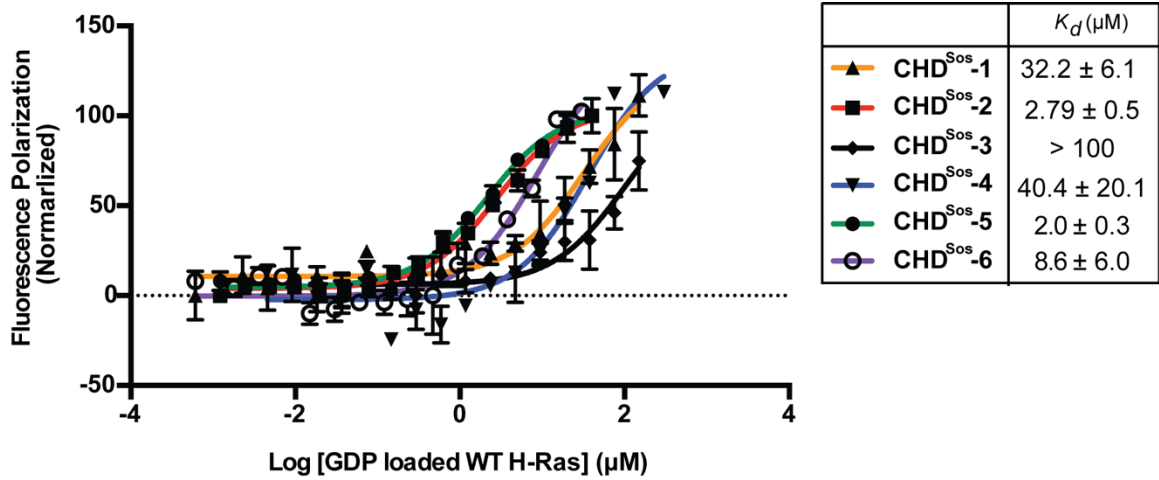


Figure S2. Fluorescence polarization curves for binding of fluorescently-labeled CHDs and GDP-bound wild-type H-Ras. The calculated dissociation constants (K_d) for each CHD are listed in the Table. Error bars are mean \pm SD of triplicates.

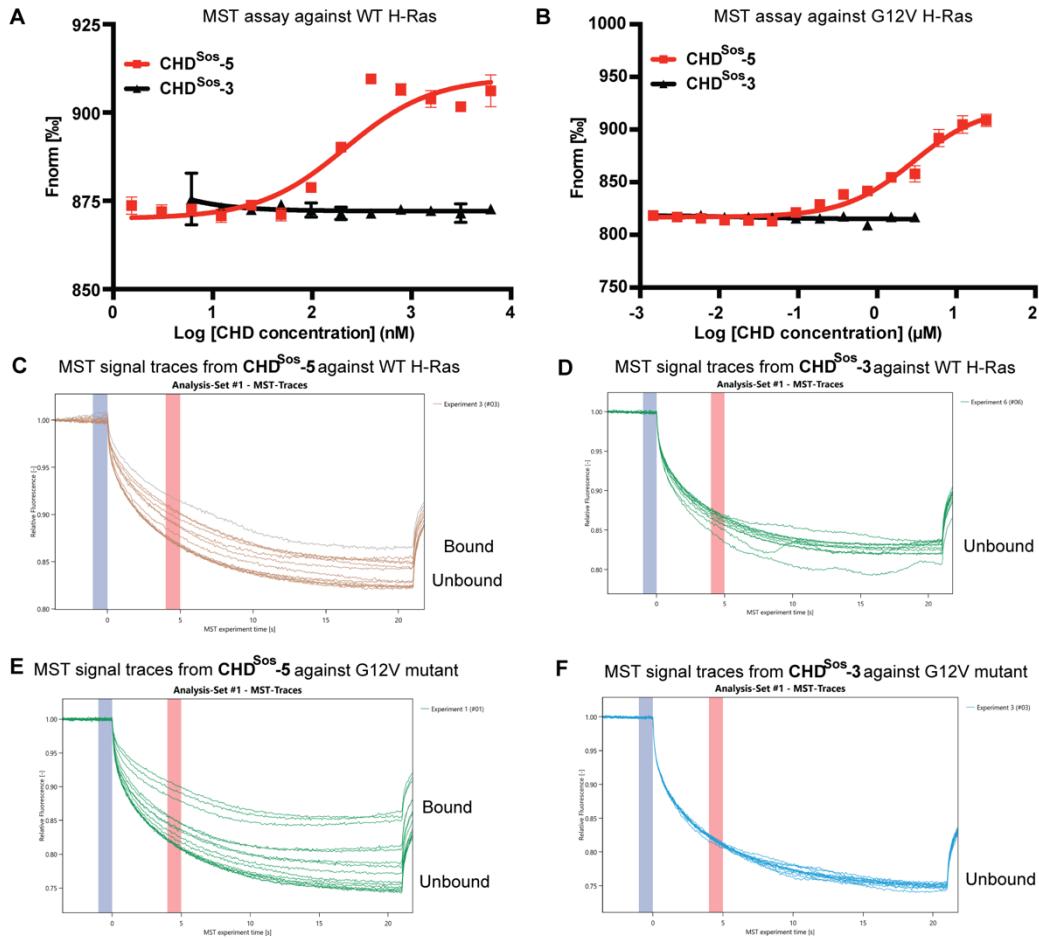


Figure S3. Microscale thermophoresis analysis of CHD binding with and wild-type and mutant H-Ras labeled with AFDye 647. A) Dose-response curve for interaction between CHD^{Sos-5} and CHD^{Sos-3} and wild-type H-Ras-GDP. (B) Dose-response curve for interaction between CHD^{Sos-5} and CHD^{Sos-3} and G12V H-Ras-GDP. Changes in TRIC signal observed from microscale thermophoresis are plotted as Fnorm vs. Ligand concentrations. Thermographs of wild-type H-Ras-GDP binding to (C) CHD^{Sos-5} and (D) CHD^{Sos-3}. Aggregation was observed with CHD^{Sos-3} at concentration higher than 3 μM and interrupted binding isotherm. Thermographs of G12V H-Ras-GDP binding to (E) CHD^{Sos-5} and (F) CHD^{Sos-3}. Cold region (blue) is set to 0 sec and hot region (red) at 3 sec are used. Error bars are mean ± SD from triplicates.

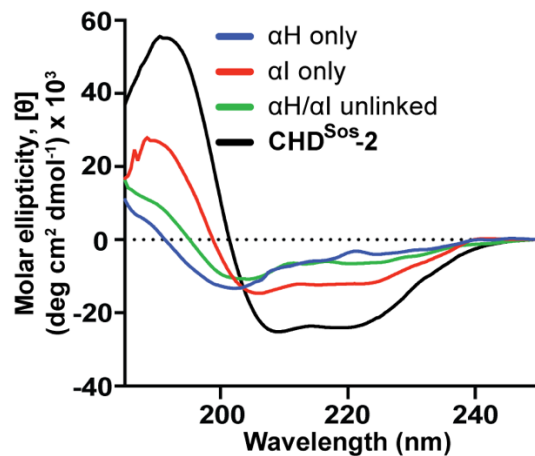


Figure S4. Circular dichroism spectra of crosslinked and linear peptides. CD spectra of the individual unlinked α H and α I peptides, equimolar mixture of the α H and α I peptides, and the **CHD^{Sos}-2**. CD experiments were conducted in 50 mM aqueous potassium fluoride buffer (pH 7.5) with 20 μ M peptide concentration.

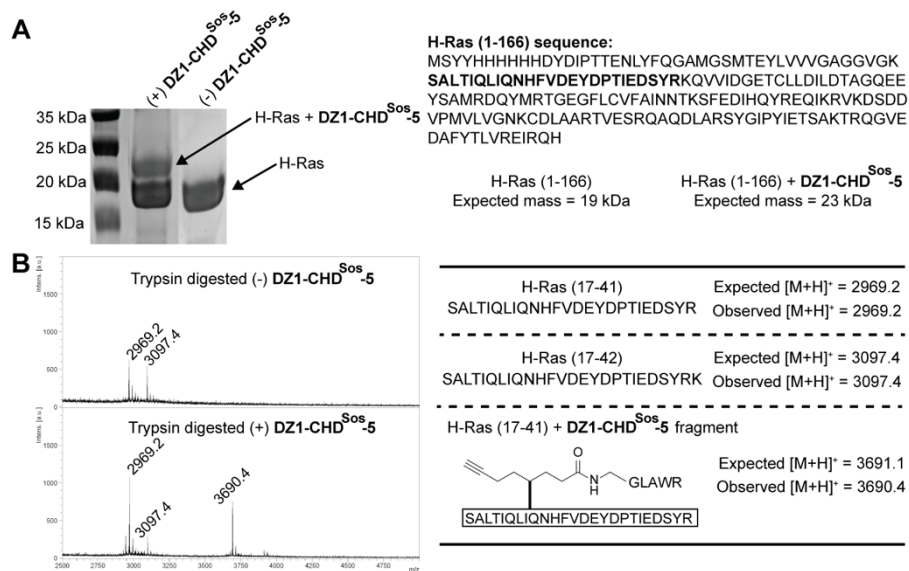


Figure S6. Chemical crosslinking of diazirine-modified CHD^{Sos}-5 supports Ras binding site. (A) Gel shift assay with H-Ras incubated with and without **DZ1-CHD^{Sos}-5**. (B) MALDI-TOF spectra displaying identified fragment masses of trypsin-digested **DZ1-CHD^{Sos}-5** crosslinked to the Ras switch I loop. Corresponding labeled mass was not observed from the unlabeled Ras sample.

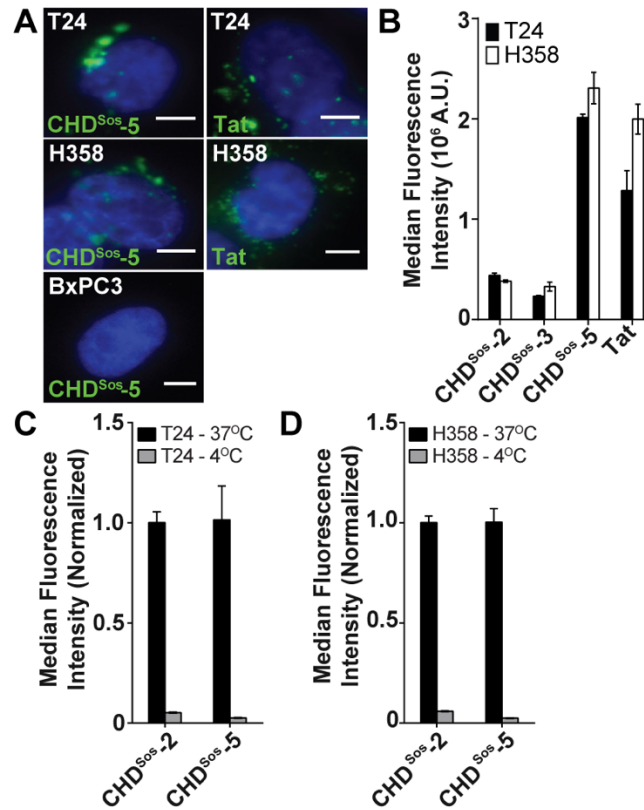


Figure S7. Fluorescence microscopy and flow cytometry studies to analyze cellular uptake of CHDs. (A) Live cell fluorescence imaging of Hoechst-stained Ras mutant T24, H358, and BxPC3 cells incubated with fluorescently-labeled peptides and DMSO (negative control) for 4 hours at 40X (scale bar = 5 μ m) magnification. Cells were exposed to 500 nM of CHDs and Tat. (B) Median fluorescence intensities in T24 and H358 cells post-treatment with 1 μ M **CHD^{Sos-2}**, **CHD^{Sos-3}**, and **CHD^{Sos-5}** and Tat for 1 hour. (C) Flow cytometry analysis of fluorescently labeled **CHD^{Sos-5}** (1 μ M) in indicated cell lines after 1 h treatment. (D) Error bars are mean \pm SD of biological duplicates.

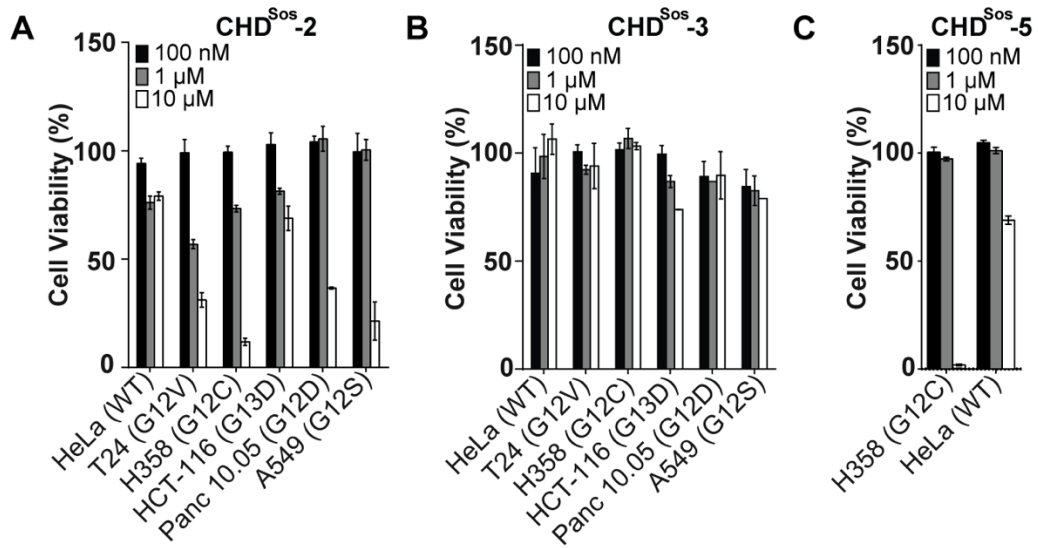


Figure S8. MTT and CellTiter-Glo assays to determine cell viability in the presence of CHDs. MTT cell viability in indicated Ras mutant and control cell lines treated with increasing concentrations of (A) **CHD^{Sos}-2** and (B) **CHD^{Sos}-3**. The cell viability studies were performed in the presence of serum. (C) Cell viability assessed by CellTiter-Glo assay in H358 and HeLa cells treated with increasing concentrations of **CHD^{Sos}-5**. Error bars are mean \pm SD of biological triplicates.

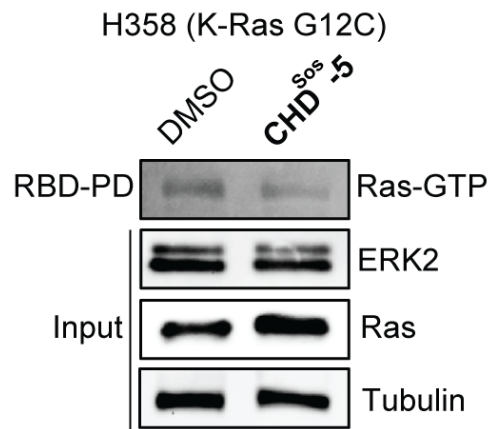


Figure S9. Representative Western blots to probe the effect of CHD^{Sos}-5 on the levels of active/GTP-bound Ras. Ras-GTP levels were determined by immunoblotting with Ras-GTP-specific antibody after treatment of H358 cells with 10 μ M CHD^{Sos}-5 for 6 hours.

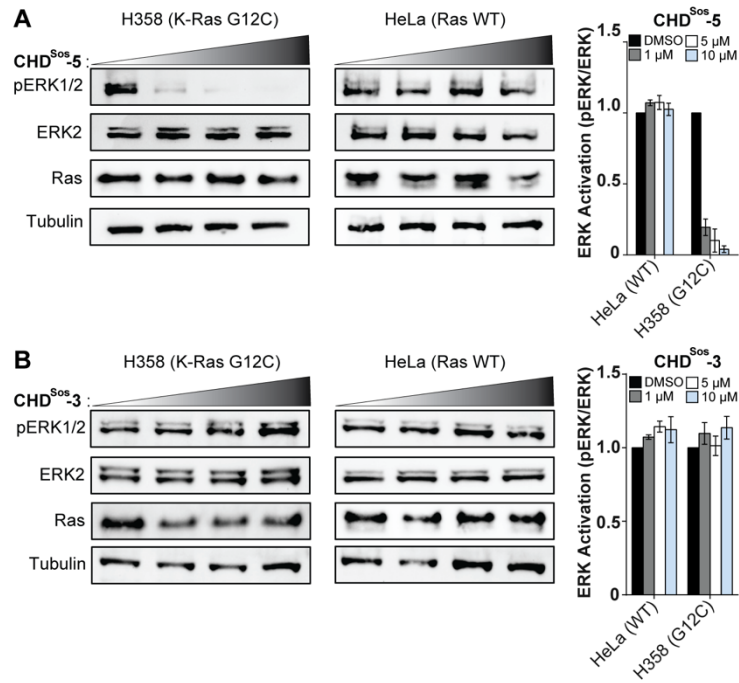


Figure S10. Representative Western blots to analyze ERK phosphorylation. Suppression of ERK phosphorylation by CHDs was probed in H358 and HeLa cells after treatment with (A) CHD^{Sos}-5 and (B) CHD^{Sos}-3 (DMSO, 1, 5, 10 μM). Error bars are mean ± SD of biological duplicates.

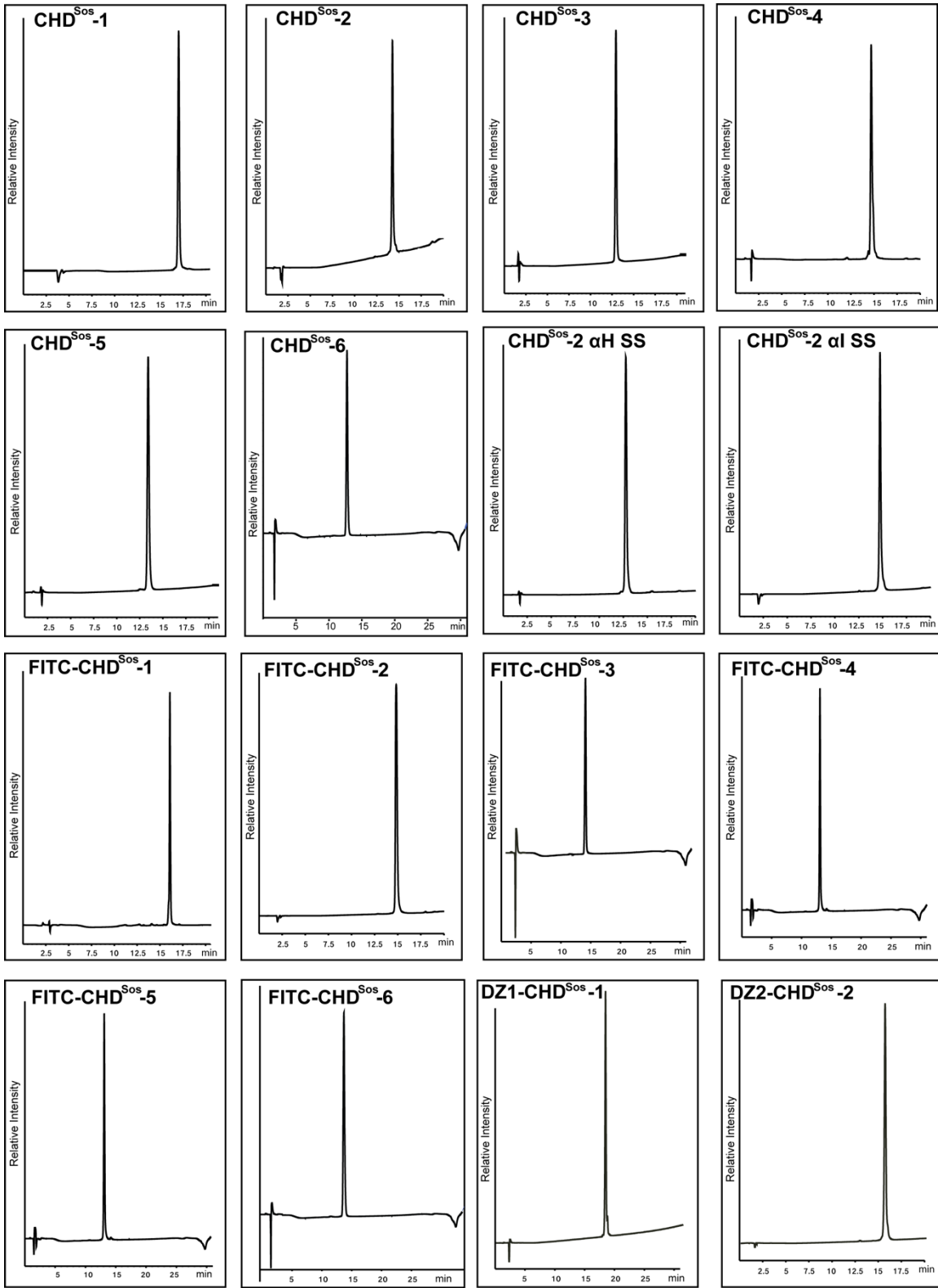
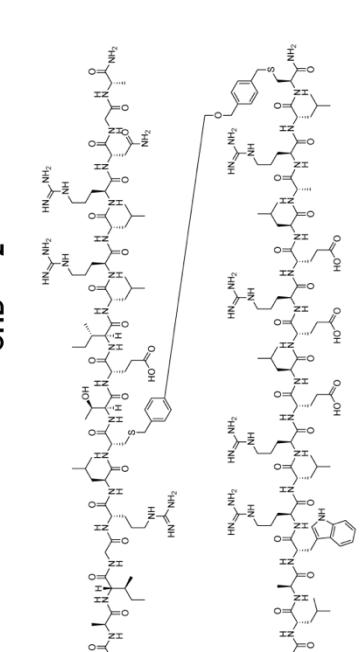
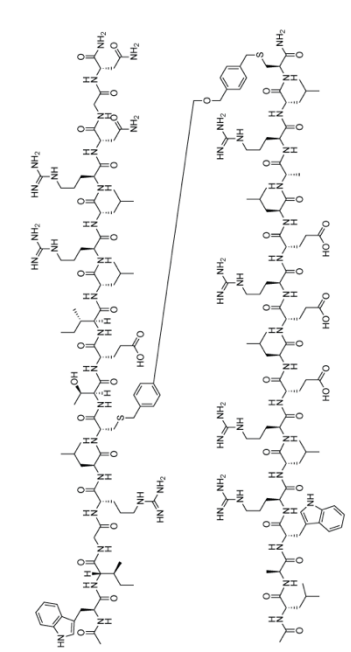
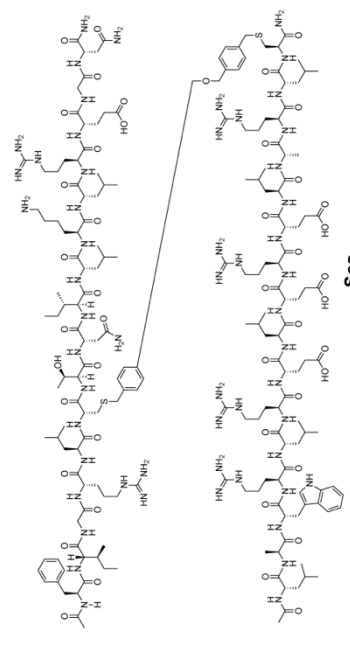
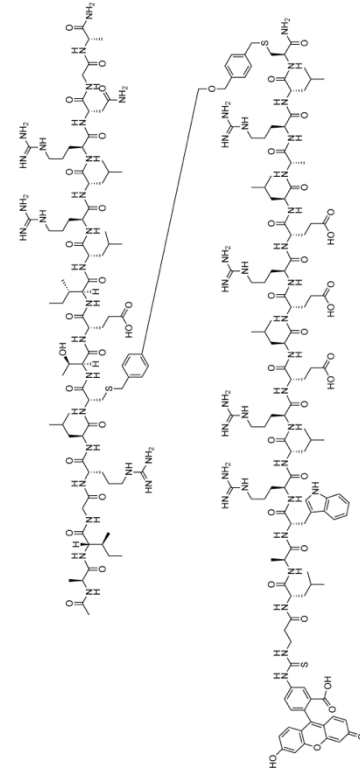
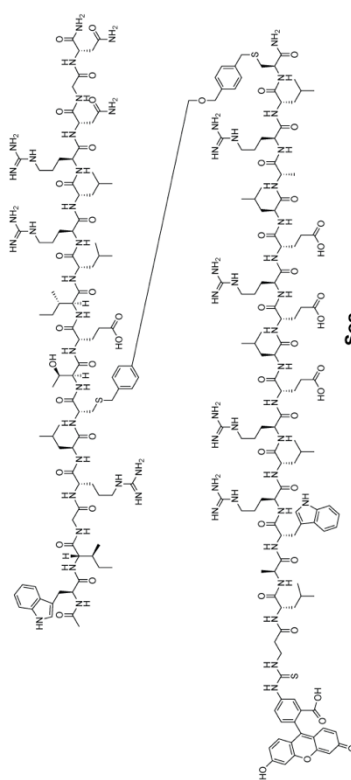
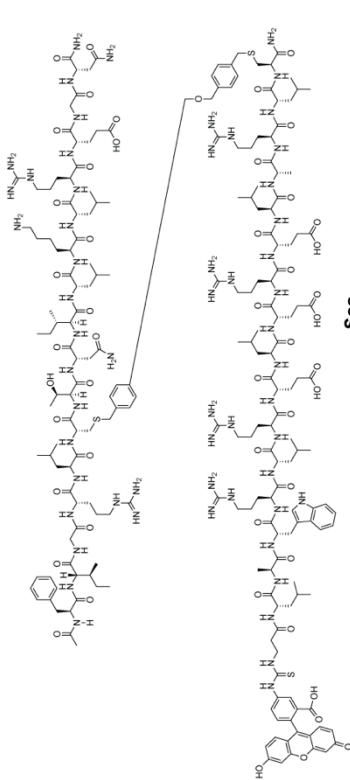
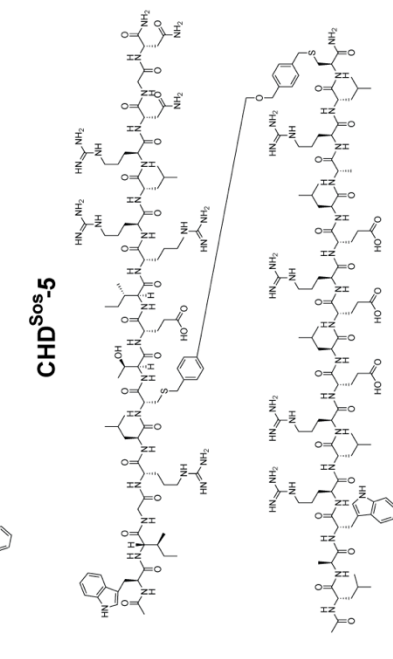
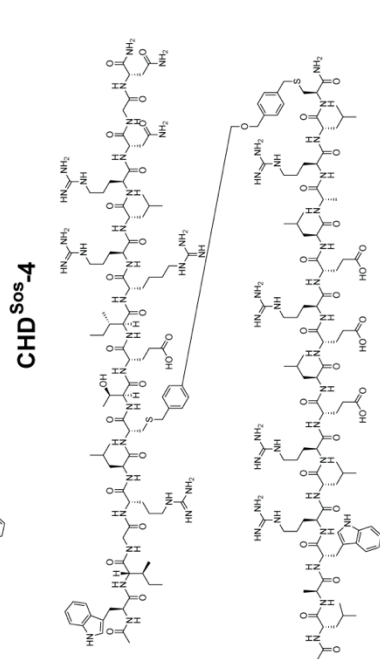
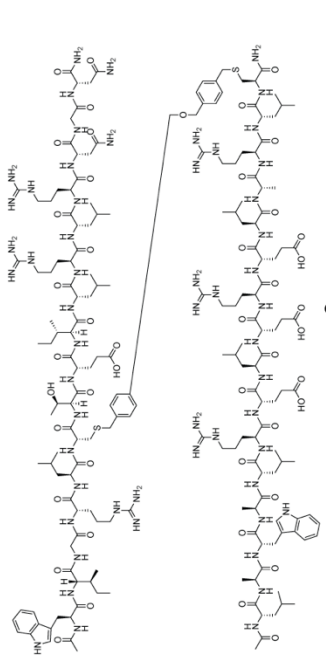
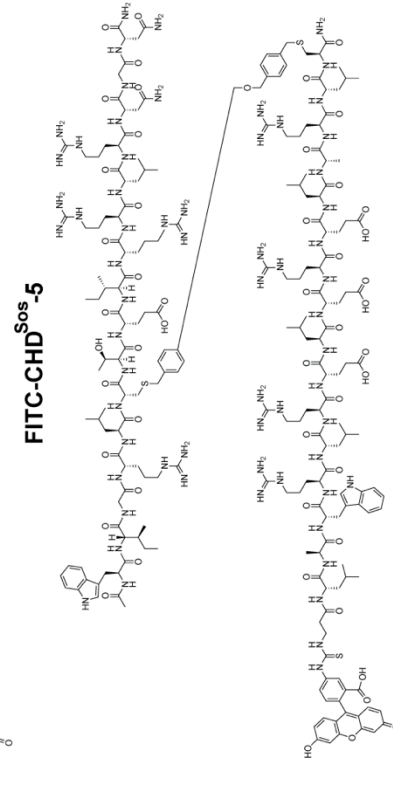
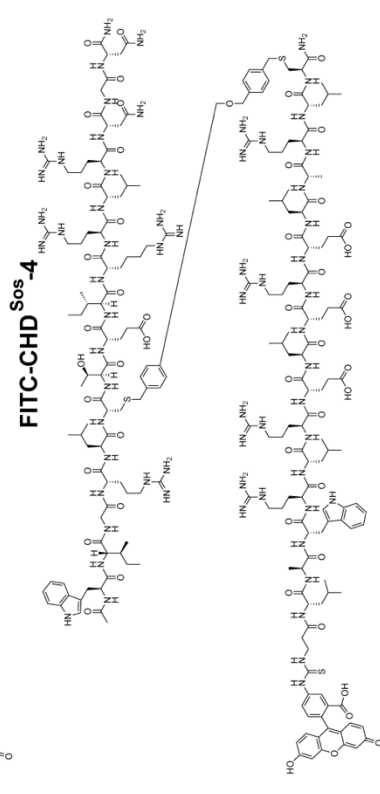
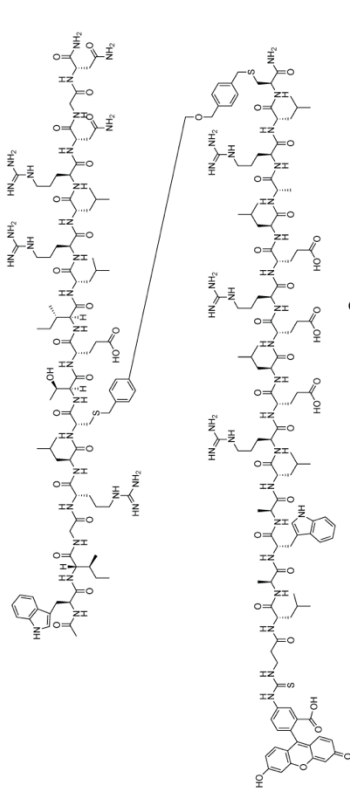


Figure S11. Analytical HPLC traces of purified linear and CHD peptides.





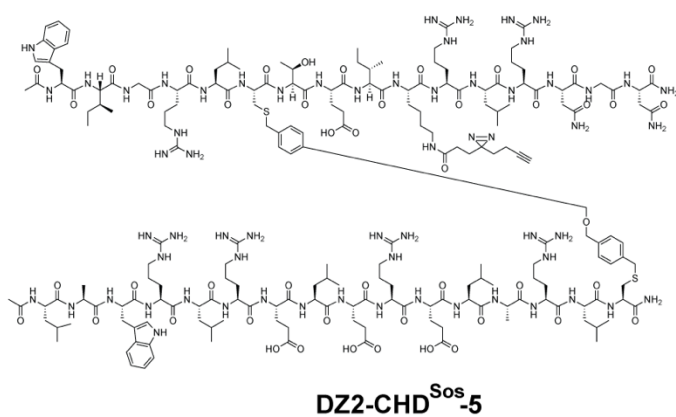
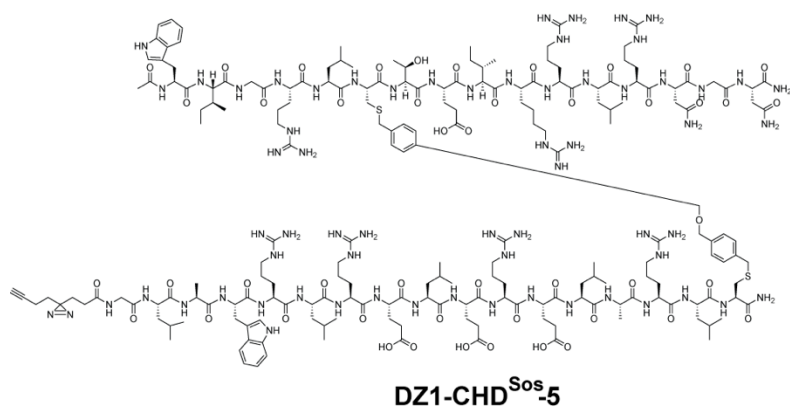
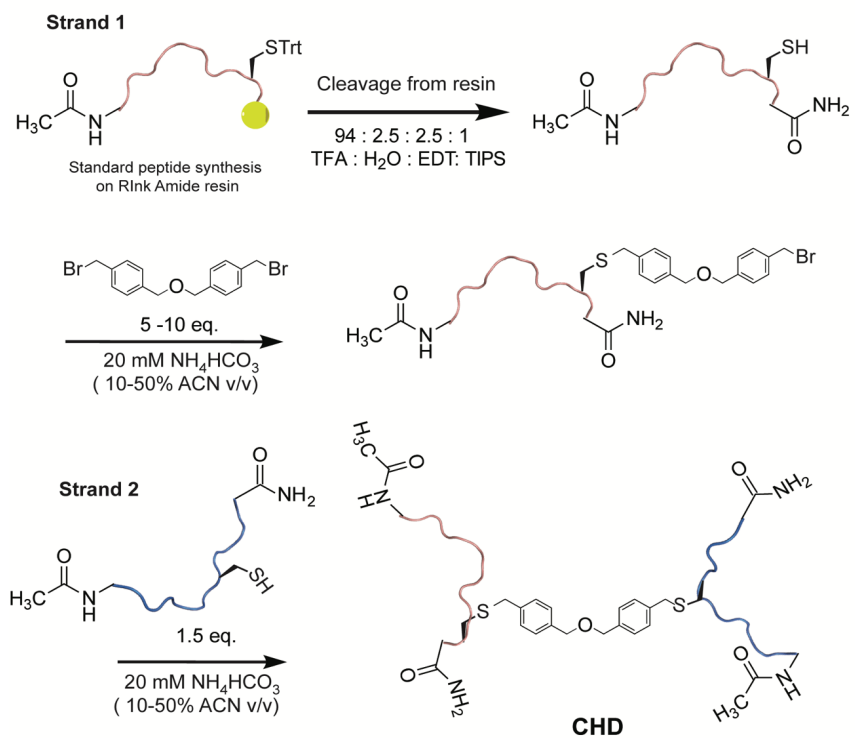


Figure S12. Chemical structures of Sos CHDs.



Scheme S1. General synthetic scheme for CHD peptides.

Table S1. Computational alanine scanning for determination of hot-spot residues in the Ras-Sos complex (PDB 1NVW and 1BKD).

Sos α H Helix (929-944): FFGIYLTNILKTEEGN

Sos Residue	$\Delta\Delta G$ (kcal/mol) from 1NVW	$\Delta\Delta G$ (kcal/mol) from 1BKD
F 929	1.64	1.45
F 930	0.03	0.05
G 931	--	--
I 932	0.07	0.05
Y 933	0.01	--
L 934	0.65	0.65
T 935	1.11	1.59
R 936	0.28	0.83
I 937	--	--
L 938	0.63	0.69
K 939	0.27	0.44
T 940	-0.13	0.05
E 941	--	--
E 942	1.10	0.34
G 943	--	--
N 944	2.35	2.63

Table S2. Mass spectroscopic characterization of CHD peptides. R^H = L-homoarginine; A_β = L-β-alanine; DZ = diazirine photocrosslinker; FITC is 5-fluorescein isothiocyanate linked via thiourea bond to N-terminal amine.

Compound	Sos Domain*	Sequence	Calculated [M+H] ⁺	Observed [M+H] ⁺
CHD^{Sos-1}	Sos αH	Ac-FIGRLCTEILKLREGN-NH ₂	4180.8	4180.8
	Sos αI	Ac-LAWRLRELERELARLC-NH ₂		
CHD^{Sos-2}	Sos αH	Ac-WIGRLCTEILRLRNGN-NH ₂	4248.1	4247.0
	Sos αI	Ac-LAWRLRELERELARLC-NH ₂		
CHD^{Sos-3}	Sos αH	Ac-AIGRLCTEILRLRNGA-NH ₂	4089.9	4087.9
	Sos αI	Ac-LAWRLRELERELARLC-NH ₂		
CHD^{Sos-4}	Sos αH	Ac-WIGRLCTEILRLRNGN-NH ₂	4162.0	4162.0
	Sos αI	Ac-LAWALRELERELARLC-NH ₂		
CHD^{Sos-5}	Sos αH	Ac-WIGRLCTEIR ^H RLRNGN-NH ₂	4305.1	4304.0
	Sos αI	Ac-LAWRLRELERELARLC-NH ₂		
CHD^{Sos-6}	Sos αH	Ac-WIGRLCTEIRRLRNGN-NH ₂	4291.1	4289.5
	Sos αI	Ac-LAWRLRELERELARLC-NH ₂		
CHD^{Sos-2} αH	Sos αH	Ac-WIGRLCTEILRLRNGN-NH ₂	1957.3	1957.4
CHD^{Sos-2} αI	Sos αI	Ac-LAWRLRELERELARLC-NH ₂	2069.5	2069.4
FITC-CHD^{Sos-1}	Sos αH	Ac-FIGRLCTEILKLREGN-NH ₂	4599.2	4599.0
	Sos αI	FITC-A _β LAWRLRELERELARLC-NH ₂		
FITC-CHD^{Sos-2}	Sos αH	Ac-WIGRLCTEILRLRNGN-NH ₂	4666.5	4665.5
	Sos αI	FITC-A _β LAWRLRELERELARLC-NH ₂		
FITC-CHD^{Sos-3}	Sos αH	Ac-AIGRLCTEILRLRNGA-NH ₂	4508.3	4508.0
	Sos αI	FITC-A _β LAWRLRELERELARLC-NH ₂		
FITC-CHD^{Sos-4}	Sos αH	Ac-WIGRLCTEILRLRNGN-NH ₂	4580.4	4580.1
	Sos αI	FITC-A _β LAWALRELERELARLC-NH ₂		
FITC-CHD^{Sos-5}	Sos αH	Ac-WIGRLCTEIR ^H RLRNGN-NH ₂	4723.6	4722.3
	Sos αI	FITC-A _β LAWRLRELERELARLC-NH ₂		
FITC-CHD^{Sos-6}	Sos αH	Ac-WIGRLCTEIRRLRNGN-NH ₂	4710.6	4710.9
	Sos αI	FITC-A _β LAWRLRELERELARLC-NH ₂		
DZ1-CHD^{Sos-5}	Sos αH	Ac-WIGRLCTEIR ^H RLRNGN-NH ₂	1117.5 [M+4H] ⁴⁺	1117.6
	Sos αI	DZ-GLAWRLRELERELARLC-NH ₂		
DZ2-CHD^{Sos-5}	Sos αH	Ac-WIGRLCTEIK(DZ)RLRNGN-NH ₂	1103.3 [M+4H] ⁴⁺	1102.3
	Sos αI	Ac-LAWRLRELERELARLC-NH ₂		

*Mimic of Sos αH or αI sequence with designed changes

Table S3. Enriched proteins from MS-based proteomics using photoaffinity crosslinking of **DZ2-CHD^{Sos}-5** in H358 cells.

Accession	# Peptides	# Unique Peptides	Gene Symbol	Average Abundance		Fold	p-value	log ₂ (fold)	-log ₁₀ (p)
				DZ2-CHD ^{Sos} -5	CP-266 ^a				
P62826	11	11	RAN	7714	964	8.00	2.0E-08	3.00	7.69
P19623	7	7	SRM	1300	143	9.12	1.2E-07	3.19	6.92
P21964	7	7	COMT	1550	210	7.37	1.4E-07	2.88	6.85
P50914	6	6	RPL14	1804	284	6.36	1.8E-07	2.67	6.75
Q99497	3	3	PARK7	1518	305	4.98	1.9E-07	2.32	6.71
Q02543	7	7	RPL18A	6677	1077	6.20	2.0E-07	2.63	6.70
P51153	5	3	RAB13	198	27	7.35	2.0E-07	2.88	6.70
O75821	9	9	EIF3G	2111	276	7.64	2.2E-07	2.93	6.65
P62424	15	15	RPL7A	5704	886	6.44	2.4E-07	2.69	6.62
Q9GZZ1	7	7	NAA50	1429	201	7.11	2.6E-07	2.83	6.58
Q9H7E9	3	3	C8orf33	541	64	8.46	2.7E-07	3.08	6.57
P39019	11	11	RPS19	9543	855	11.17	3.0E-07	3.48	6.53
Q9BYD2	6	6	MRPL9	895	140	6.40	3.0E-07	2.68	6.52
Q9Y6C9	5	5	MTCH2	1152	202	5.70	3.4E-07	2.51	6.46
Q99816	9	9	TSG101	1485	174	8.53	4.4E-07	3.09	6.36
Q12765	5	5	SCRN1	625	75	8.29	5.0E-07	3.05	6.30
Q15185	8	8	PTGES3	2760	228	12.08	5.5E-07	3.59	6.26
P22087	10	10	FBL	3540	697	5.08	6.1E-07	2.34	6.21
P68104	25	13	EEF1A1	33254	3786	8.78	6.8E-07	3.13	6.17
O75608	5	5	LYPLA1	1898	368	5.16	7.1E-07	2.37	6.15
Q9H0S4	9	9	DDX47	1727	254	6.81	7.9E-07	2.77	6.10
P61026	13	10	RAB10	7046	1160	6.08	8.6E-07	2.60	6.07
P61106	14	13	RAB14	7072	1053	6.72	9.2E-07	2.75	6.04
O95470	11	11	SGPL1	717	122	5.87	9.2E-07	2.55	6.04
Q5BKZ1	3	3	ZNF326	89	14	6.21	1.3E-06	2.64	5.89
Q15691	15	15	MAPRE1	2720	360	7.55	1.3E-06	2.92	5.89
Q9BWF3	12	12	RBM4	2761	355	7.78	1.4E-06	2.96	5.86
Q08174	6	6	PCDH1	1258	157	8.00	1.4E-06	3.00	5.86
Q9BRU9	3	3	UTP23	631	141	4.47	1.4E-06	2.16	5.84
P62906	9	9	RPL10A	12200	1574	7.75	1.6E-06	2.95	5.79
Q15050	6	6	RRS1	1090	222	4.91	1.9E-06	2.30	5.71
P06493	8	8	CDK1	2291	269	8.52	2.1E-06	3.09	5.68
Q9Y3B7	6	6	MRPL11	2437	312	7.81	2.4E-06	2.97	5.62
Q14684	3	3	RRP1B	778	167	4.67	2.4E-06	2.22	5.61
P23497	5	4	SP100	453	78	5.81	2.7E-06	2.54	5.56
P38919	22	19	EIF4A3	6326	1033	6.13	2.9E-06	2.61	5.54
Q9NP72	6	6	RAB18	1628	271	6.01	3.3E-06	2.59	5.48
Q9BQA1	3	3	WDR77	67	13	5.35	3.7E-06	2.42	5.44
P62854	3	3	RPS26	743	106	6.98	3.8E-06	2.80	5.42
Q8TDB6	3	3	DTX3L	151	47	3.19	4.2E-06	1.67	5.38
Q96A08	7	3	HIST1H2BA	1514	390	3.89	5.0E-06	1.96	5.30
P39023	26	26	RPL3	13403	1468	9.13	7.7E-06	3.19	5.11
P47755	8	5	CAPZA2	521	74	7.09	8.3E-06	2.83	5.08
P36404	5	5	ARL2	665	75	8.87	9.0E-06	3.15	5.05
P52597	10	8	HNRNPF	2729	425	6.42	9.9E-06	2.68	5.01
P05787	45	37	KRT8	59794	13117	4.56	9.9E-06	2.19	5.01
P22392-2	13	5	NME2	5458	1020	5.35	1.0E-05	2.42	4.99
P52815	4	4	MRPL12	156	35	4.47	1.1E-05	2.16	4.95
P18124	17	17	RPL7	9362	1364	6.87	1.1E-05	2.78	4.94
P27707	3	3	DCK	333	51	6.51	1.2E-05	2.70	4.93
Q9H8Y8	4	4	GORASP2	202	46	4.34	1.4E-05	2.12	4.86
Q9Y496	6	6	KIF3A	399	73	5.48	1.5E-05	2.46	4.82
Q9NTK5	9	9	OLA1	1492	253	5.90	2.6E-05	2.56	4.59
Q8WYA6	12	12	CTNBL1	2201	322	6.83	2.6E-05	2.77	4.58
P09493-3	16	5	TPM1	2215	527	4.20	3.0E-05	2.07	4.52
P60660	6	6	MYL6	2017	395	5.10	3.3E-05	2.35	4.49
Q5JWF2	5	4	GNAS	104	19	5.62	3.3E-05	2.49	4.48
Q9GZZ9	3	3	UBA5	413	51	8.06	3.4E-05	3.01	4.47
P09211	8	8	GSTP1	4548	947	4.80	5.1E-05	2.26	4.29
Q96FQ6	4	4	S100A16	2466	426	5.79	6.1E-05	2.53	4.21

Q9H7Z7	14	14	PTGES2	4174	521	8.01	6.6E-05	3.00	4.18
P17931	6	6	LGALS3	2583	517	4.99	6.7E-05	2.32	4.17
O00299	8	8	CLIC1	3016	340	8.88	6.8E-05	3.15	4.16
O60506-3	28	23	SYNCRIP	16364	2845	5.75	7.3E-05	2.52	4.14
Q13243	5	4	SRSF5	553	145	3.81	8.0E-05	1.93	4.10
Q8TDD1	9	9	DDX54	1424	405	3.52	8.9E-05	1.81	4.05
Q9BTY7	4	4	HGH1	506	93	5.45	9.5E-05	2.45	4.02
P27144	5	5	AK4	1250	154	8.11	1.1E-04	3.02	3.97
P54819	6	6	AK2	1082	335	3.23	1.1E-04	1.69	3.94
P45973	6	6	CBX5	4248	832	5.11	1.2E-04	2.35	3.92
Q9UNX4	5	5	WDR3	235	72	3.24	1.3E-04	1.69	3.88
Q5T6V5	5	5	C9orf64	420	55	7.71	1.5E-04	2.95	3.83
Q07666	12	12	KHDRBS1	9696	1587	6.11	1.7E-04	2.61	3.76
Q15785	9	9	TOMM34	1723	156	11.08	2.4E-04	3.47	3.61
Q9BVP2	12	12	GNL3	2113	441	4.80	2.7E-04	2.26	3.57
Q9BVI4	5	5	NOC4L	366	73	5.03	2.9E-04	2.33	3.54
Q9BQ67	5	5	GRWD1	1045	311	3.36	3.0E-04	1.75	3.52
Q9Y2X3	10	10	NOP58	2414	869	2.78	3.1E-04	1.47	3.51
P56182	7	7	RRP1	680	174	3.91	3.2E-04	1.97	3.50
O60841	10	10	EIF5B	689	158	4.37	3.2E-04	2.13	3.49
P54619	9	9	PRKAG1	3113	336	9.27	3.5E-04	3.21	3.45
Q8WUA2	3	3	PPIL4	189	33	5.66	3.5E-04	2.50	3.45
P01116-2	6	6	KRAS	825	124	6.63	3.7E-04	2.73	3.43
Q9BRK5	6	6	SDF4	633	90	7.02	3.9E-04	2.81	3.41
Q9Y3D6	3	3	FIS1	357	126	2.84	4.2E-04	1.51	3.37
P31146	5	4	CORO1A	523	117	4.47	5.6E-04	2.16	3.25
P62280	9	9	RPS11	6290	579	10.86	5.6E-04	3.44	3.25
Q15070	4	4	OXA1L	186	37	5.08	5.6E-04	2.34	3.25
Q8IY81	15	15	FTSJ3	2367	788	3.01	5.7E-04	1.59	3.24
Q08257	4	4	CRYZ	254	70	3.61	5.7E-04	1.85	3.24
Q14137	6	6	BOP1	631	163	3.87	5.8E-04	1.95	3.23
Q9NVP1	16	16	DDX18	2793	821	3.40	6.2E-04	1.77	3.21
O96008	8	8	TOMM40	3359	735	4.57	6.3E-04	2.19	3.20
Q86SX6	3	3	GLRX5	357	85	4.21	6.3E-04	2.07	3.20
P46777	11	11	RPL5	6090	837	7.27	6.6E-04	2.86	3.18
P35080-2	4	3	PFN2	1570	232	6.76	7.1E-04	2.76	3.15
Q10713	4	4	PMPCA	395	100	3.94	7.3E-04	1.98	3.14
P62851	5	5	RPS25	5841	577	10.13	7.8E-04	3.34	3.11
P06753-2	24	12	TPM3	16084	3226	4.99	8.4E-04	2.32	3.08
Q8WU90	9	9	ZC3H15	270	39	6.94	9.6E-04	2.79	3.02
Q8NEJ9	3	3	NGDN	251	45	5.53	1.1E-03	2.47	2.96
Q99614	6	6	TTC1	1189	183	6.51	1.1E-03	2.70	2.94
P28066	6	6	PSMA5	2172	340	6.39	1.2E-03	2.68	2.94
P30419	4	4	NMT1	480	165	2.90	1.4E-03	1.54	2.86
Q13206	3	3	DDX10	87	19	4.64	1.4E-03	2.22	2.84
P05783	31	30	KRT18	34924	9662	3.61	1.5E-03	1.85	2.83
P31943	14	8	HNRNPH1	11191	1588	7.05	1.5E-03	2.82	2.82
O75844	4	4	ZMPSTE24	1308	482	2.71	1.6E-03	1.44	2.80
P27635	10	10	RPL10	8043	984	8.18	1.7E-03	3.03	2.78
P62258	22	20	YWHAE	16731	1848	9.05	1.7E-03	3.18	2.76
Q9BUQ8	5	5	DDX23	207	68	3.05	1.8E-03	1.61	2.75
P60842	25	13	EIF4A1	13939	1642	8.49	1.8E-03	3.09	2.74
Q9H074	3	3	PAIP1	276	45	6.18	1.8E-03	2.63	2.74
P61981	10	6	YWHAG	2231	261	8.53	2.0E-03	3.09	2.70
P63241	10	10	EIF5A	5906	792	7.46	2.0E-03	2.90	2.69
Q13247	6	5	SRSF6	2200	666	3.30	2.0E-03	1.72	2.69
Q9H3Q1	4	4	CDC42EP4	535	48	11.13	2.1E-03	3.48	2.68
P27348	14	9	YWHAQ	5706	648	8.81	2.1E-03	3.14	2.68
P82930	3	3	MRPS34	717	101	7.08	2.2E-03	2.82	2.67
Q14498	6	6	RBM39	1230	425	2.90	2.2E-03	1.53	2.66
O76021	20	20	RSL1D1	5114	1655	3.09	2.3E-03	1.63	2.64
O95758-1	8	5	PTBP3	333	55	6.06	2.5E-03	2.60	2.61
Q6P1J9	3	3	CDC73	251	58	4.34	2.5E-03	2.12	2.60
Q53GQ0	10	10	HSD17B12	3717	495	7.51	2.6E-03	2.91	2.59
Q9HAV4	4	4	XPO5	197	49	3.98	2.8E-03	1.99	2.55
Q96S44	4	4	TP53RK	596	52	11.54	3.0E-03	3.53	2.53
P0DP25	5	5	CALM3	1088	211	5.16	3.2E-03	2.37	2.50
Q9ULX3	3	3	NOB1	233	23	9.99	3.2E-03	3.32	2.49

P19338	42	42	NCL	21643	8238	2.63	3.3E-03	1.39	2.49
P78318	6	6	IGBP1	660	74	8.91	3.3E-03	3.16	2.48
Q05639	22	10	EEF1A2	4035	438	9.22	3.3E-03	3.20	2.48
P24534	9	7	EEF1B2	6809	646	10.55	3.4E-03	3.40	2.47
P19784	7	7	CSNK2A2	812	112	7.25	3.5E-03	2.86	2.46
Q9ULC4	4	4	MCTS1	484	82	5.88	3.5E-03	2.56	2.45
Q96A49	11	11	SYAP1	966	109	8.88	3.7E-03	3.15	2.43
Q99439	6	4	CNN2	791	186	4.24	3.8E-03	2.09	2.42
Q15628	4	4	TRADD	74	17	4.34	4.0E-03	2.12	2.39
O60547	5	5	GMDS	261	32	8.12	4.1E-03	3.02	2.38
P04632	6	6	CAPNS1	555	87	6.35	4.2E-03	2.67	2.37
P40939	22	22	HADHA	4549	1190	3.82	4.5E-03	1.94	2.35
Q9BYG3	5	5	NIFK	1813	344	5.27	4.8E-03	2.40	2.32
Q01081	4	4	U2AF1	396	85	4.66	4.8E-03	2.22	2.32
P49720	3	3	PSMB3	422	159	2.66	5.2E-03	1.41	2.28
Q9BUF5	18	8	TUBB6	2620	284	9.22	5.2E-03	3.21	2.28
P61224	3	3	RAP1B	1520	227	6.69	5.6E-03	2.74	2.25
P35659	11	11	DEK	2440	785	3.11	5.7E-03	1.64	2.25
P20042	12	12	EIF2S2	5270	893	5.90	5.8E-03	2.56	2.24
Q99747	6	6	NAPG	98	18	5.47	6.2E-03	2.45	2.20
P35222	17	15	CTNNB1	4435	1217	3.64	6.4E-03	1.87	2.20
Q96FW1	7	7	OTUB1	3921	446	8.79	6.5E-03	3.14	2.18
Q01105	12	3	SET	5660	1233	4.59	6.6E-03	2.20	2.18
P55795	10	5	HNRNPH2	1682	230	7.30	6.6E-03	2.87	2.18
P51148	8	6	RAB5C	2640	450	5.87	6.7E-03	2.55	2.17
P61081	6	6	UBE2M	1401	229	6.13	6.7E-03	2.62	2.17
Q9P2K5	4	4	MYEF2	262	44	5.98	6.8E-03	2.58	2.17
Q99829	3	3	CPNE1	215	35	6.17	6.9E-03	2.62	2.16
Q9P287	4	4	BCCIP	693	94	7.38	6.9E-03	2.88	2.16
Q92733	5	5	PRCC	893	160	5.59	7.0E-03	2.48	2.15
Q9BX10	3	3	GTPBP2	91	11	8.15	7.1E-03	3.03	2.15
P50402	10	10	EMD	3191	480	6.64	7.2E-03	2.73	2.14
O14773	3	3	TPP1	113	32	3.49	7.4E-03	1.80	2.13
Q99627	4	4	COPS8	1199	190	6.31	7.6E-03	2.66	2.12
P39687	9	4	ANP32A	2059	284	7.26	7.9E-03	2.86	2.10
P09651	18	13	HNRNPA1	10688	2198	4.86	8.0E-03	2.28	2.10
P30484	7	4	HLA-B	415	86	4.85	8.3E-03	2.28	2.08
P63104	18	13	YWHAZ	16707	1983	8.42	8.4E-03	3.07	2.07
O43390	27	22	HNRNPR	10264	1745	5.88	8.6E-03	2.56	2.07
P29692	10	8	EEF1D	6725	614	10.95	9.0E-03	3.45	2.04
Q9P289	9	5	STK26	1337	170	7.87	9.3E-03	2.98	2.03
P60510	3	3	PPP4C	377	60	6.27	9.8E-03	2.65	2.01
Q15126	8	8	PMVK	1594	177	9.02	9.9E-03	3.17	2.00
O95433	12	12	AHSA1	1074	157	6.84	9.9E-03	2.77	2.00

^aCP-266 = 3-(3-(but-3-yn-1-yl)-3H-diazirin-3-yl)-N-methylpropanamide

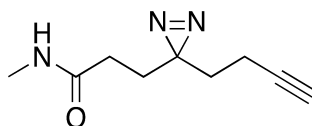


Table S4A. Analysis of sequence similarity within enriched Ras GTPase proteins as compared to K-Ras.

Accession	Gene Symbol	G-Domain (Residues 1-166)		Switch I + Binding Helix (Residues 10-40)		Switch II (Residues 56-75)	
		% Identity	% Similarity	% Identity	% Similarity	% Identity	% Similarity
P01116-2	KRAS	-	-	-	-	-	-
P62826	RAN	25.9	68.1	25.8	67.7	45	75
P51153	RAB13	38.0	75.3	35.5	71.0	40	70
P61026	RAB10	35.5	73.5	25.8	64.5	40	70
P61106	RAB14	31.3	69.9	35.5	64.5	45	70
Q9NP72	RAB18	33.7	71.1	35.5	64.5	40	70
P61224	RAP1B	57.2	88.0	74.2	96.8	65	90
P51148	RAB5C	31.9	72.9	29.0	77.4	45	65
P01112	HRAS	94.0	98.8	100	100	100	100
P01111	NRAS	94.0	98.2	100	100	100	100

Table S4B. Analysis of sequence similarity within enriched non-Ras G-proteins as compared to K-Ras.

Accession	Gene Symbol	G-Domain (Residues 1-166)		Switch I + Binding Helix (Residues 10-40)		Switch II (Residues 56-75)	
		% Identity	% Similarity	% Identity	% Similarity	% Identity	% Similarity
P01116-2	KRAS	-	-	-	-	-	-
Q5JWF2	GNAS	41	62	10	8	4	6
P36404	ARL2	23.0	58.0	6.0	15.0	4	9
Q9BX10	GTPBP2	13.3	44.0	22.6	54.8	20	40
P19784	CSNK2A2	21.1	52.4	6.5	12.9	10	15
Q9BVP2	GNL3	19.9	49.4	22.6	51.6	5	25
O60841	EIF5B	22.3	56.6	25.8	58.1	30	65
Q9NTK5	OLA1	24.1	60.2	29.0	58.1	15	55